Photooxidation of Cinnamaldehyde in Methanol — Product Analysis and Evolving Factor Analysis of UV Spectra

M. ČEPPAN, R. FIALA, V. BREZOVÁ, J. PANÁK, and V. MOTLÍKOVÁ

Department of Printing Technology and Applied Photochemistry, Faculty of Chemical Technology, Slovak Technical University, SK-812 37 Bratislava

Received 25 October 1993

The photooxidation of cinnamaldehyde in methanol was studied by GC/MS, TLC, and UV absorption spectroscopy in the $\lambda = 200$—350 nm region. TLC indicates four components of the reaction mixtures. These components were identified by GC/MS as *trans*- and *cis*-cinnamaldehyde and *trans*- and *cis*-dimethyl acetal of cinnamaldehyde. Set of the UV absorption spectra of the photooxidation reaction mixtures was analyzed by the Evolving Factor Analysis. Three spectra of components were isolated and the compositions of the reaction mixtures were determined. The isolated spectra correspond to *trans*- and *cis*-cinnamaldehyde and dimethyl acetal of cinnamaldehyde. On the basis of the determined compositions of reaction mixtures Principal Components Regression calibration model of the UV spectra set was developed.

Aromatic aldehydes are known to undergo various photochemical reactions in both gaseous and liquid phases. The self deactivation of an excited aldehyde RCHO* by a ground state aldehyde molecule RCHO associated with the hydrogen transfer

$$\mathrm{RCHO^* + RCHO \rightarrow R\dot{C}HOH + R\dot{C}O} \qquad (A)$$

is the initiation stage of aldehydes photooxidation in solutions [1]. Both radicals interact with dioxygen giving peroxy radicals. In the case of benzaldehyde photooxidation in alcohols these peroxy radicals open chain reactions producing peroxybenzoic acid [2]. On the other hand, a corresponding diacetal was found to be the product of *p*-isothiocyanatobenzaldehyde photooxidation in alcohols [3].

This paper deals with the photooxidation of 3-phenyl-2-propenal (cinnamaldehyde) in methanol and presents the results of the product analysis and the Evolving Factor Analysis of the UV spectra recorded in the course of the photooxidation.

EXPERIMENTAL

Cinnamaldehyde (Lobachemie, Austria) was purified by vacuum distillation [4]. Pure cinnamaldehyde was stored in a freezer under nitrogen atmosphere.

Methanol for UV spectroscopy grade (Lachema, Brno) dried over anhydrous Na_2SO_4 and distilled was used for all preparations of cinnamaldehyde solutions.

Thin-layer chromatography (TLC) was performed on silica gel plates Silufol UV 254 (Kavalier, Votice). Plates were activated for 15 min at 100 °C prior to use. Mixture of n-hexane and diethyl ether ($\varphi_r = 1 : 1$, both anal. grade, Lachema, Brno) was used as mobile phase.

UV spectra were recorded on PU8800 UV VIS spectrophotometer (Philips Analytical, Cambridge, UK). Spectra digitized in 120 points were put into computations.

GC/MS analysis was performed on HP 59800A/5790 Chemstation (Hewlett—Packard).

Photoisomerization and photooxidation experiments were performed at the temperature 15 °C in immersion well quartz photochemical reactor (Applied Photophysics, London, UK). The studied systems were irradiated by the polychromatic light of a medium pressure mercury 125 W lamp.

COMPUTATIONS

Factor analysis is a computational tool for solving multidimensional problems which has been implemented in several areas of analytical spectroscopy [5—7]. According to Beer's law spectral data matrix $\boldsymbol{A}$ can be decomposed into the product of a molar absorptivity matrix $\boldsymbol{S}$ and concentration matrix $\boldsymbol{C}$

$$\boldsymbol{A} = \boldsymbol{SC} \qquad (1)$$

Spectral vectors $\boldsymbol{a}_j$ of the N_S chemical mixtures under study are in the columns of $\boldsymbol{A}$ (dimension $N_W \times N_S$). Each spectral vector is formed from N_W elements of digitized spectrum. The columns of $\boldsymbol{S}$ (dimension $N_W \times N_C$) are formed by the spectral vectors $\boldsymbol{s}_k$ of the N_C chemical components and the rows of $\boldsymbol{C}$ (dimension $N_C \times N_S$) by their concentration vectors; each concentration vector consists of corresponding components concentrations in N_S mixtures.

The task of the spectrometric analysis is to decompose spectral data matrix $\boldsymbol{A}$ into the product (*1*).

Abstract Factor Analysis (AFA) performs related decomposition (abstract decomposition) yielding an eigenvectors matrix $\boldsymbol{Q}$ (abstract spectra matrix), factor matrix $\boldsymbol{U}$ (abstract concentration matrix), and a diagonal matrix Λ of the eigenvalues of the covariance matrix $\boldsymbol{Z}$

$$\boldsymbol{A} = \boldsymbol{QU} \tag{2}$$

$$\boldsymbol{Z} = \boldsymbol{AA}^T \tag{3}$$

According to the theory of errors in AFA [8] both eigenvectors and eigenvalues can be classified as primary (displaying predominantly chemical information involved in spectral data matrix) and secondary (displaying exclusively experimental errors of spectral data). Thus primary eigenvectors constitute an orthonormal basis of the primary factor spectral space with the dimension equal to the number of components. Real error of the spectral data is evaluated as

$$RE(N_C) = \sqrt{\frac{1}{N_W(N_S - N_C)} \sum_{k=N_C+1}^{N_S} \lambda_k^\circ} \tag{4}$$

where summation runs through secondary eigenvalues λ_k°. RE is a measure of the experimental error reproduction in the N_C dimensional factor spectral space. The $RE(N_C)$ is significantly higher than true experimental error if the dimension of the factor space was underestimated, *i.e.* true number of components is higher than N_C used in eqn (*4*). On the contrary satisfying reproduction of experimental error, *i.e.* $RE(N_C)$ close to the true experimental error, indicates the coincidence of N_C with the true number of components.

The relation between abstract factor solution (*3*) and true spectra and concentrations of components is given by the transformations

$$\boldsymbol{S} = \boldsymbol{QT} \tag{5}$$

$$\boldsymbol{C} = \boldsymbol{T}^{-1}\boldsymbol{U} \tag{6}$$

Evolving Factor Analysis (EFA) [9—11] is a technique which allows the calculation of concentration profiles and component spectra from the spectra set exhibiting an intrinsic order. Examples of such intrinsic ordered spectra sets are spectra of mixtures evolving in correspondence with the changes of the equilibrium concentrations of components, spectra sets of various spectrophotometric titrations, multiwavelength chromatograms and as in this paper spectra of reaction mixtures scanned in certain intervals of the reaction course. According to the concept of EFA the quantitative structure of a spectral set correlates with the structure of eigenvalues of the matrix $\boldsymbol{Z}$. Evolution of this structure reflects the evolution of the system under study.

EFA algorithm [9] consists of two parts. In the first of them (primary EFA) AFA is successively performed with the subsets of the first N_C, $N_C + 1$, up to $N_S - N_C + 1$ spectra and corresponding sets of eigenvalues $(\lambda_k)_F^j$ ($k = 1 \rightarrow N_C$) are obtained for every such spectral subset $j = N_C \rightarrow N_S - N_C + 1$. The primary eigenvalues of this forward primary EFA emerge from the level of secondary eigenvalues as new components in the spectra appear during the evolution of the system. The backward primary EFA performs a similar procedure starting with the last N_C spectra (*i.e.* spectra N_S, $N_S - 1$, ..., $N_S - N_C + 1$) and successively adds the spectra $(N_S - N_C)$, $(N_S - N_C - 1)$ up to the spectrum N_C into the AFA analyzed subsets. The primary eigenvalues of the backward EFA $(\lambda_k)_B^j$ correspond to the disappearance of the components. The eigenvalues sets of both the forward and backward primary EFA are plotted together as a function of the evolution. The concentration profile of the k-th component is then found as the boundaries of the area under the curves of the i-th forward and $(N_C + 1 - k)$-th backward eigenvalues plot, *i.e.*

$$p_{kj} = \min\{(\lambda_k)_F^j; (\lambda_{N_C+1-k})_B^j\} \tag{7}$$

The key feature of EFA is the concentration window for each component [9], *i.e.* the definition of significant and insignificant eigenvalues in every row of the concentration profiles matrix $\boldsymbol{P}$. Component concentration window then provides a range of existence of the component in the course of the evolution of the system. Outside this window the component is assumed to be not present, its concentration is therefore zero.

The second part of EFA (iterative EFA) essentially performs the transformations (*5*), (*6*) by an iterative refinement of the concentration profiles by normalization, calculation of the spectra from normalized concentrations $\boldsymbol{P}^*$

$$\boldsymbol{S} = \boldsymbol{AP}^{*T}\{\boldsymbol{P}^*\boldsymbol{P}^{*T}\}^{-1} \tag{8}$$

and recalculation of the concentration profiles from $\boldsymbol{S}$

$$\boldsymbol{P} = \{\boldsymbol{S}^T\boldsymbol{S}\}^{-1}\boldsymbol{S}^T\boldsymbol{A} \tag{9}$$

In each step physically incorrect negative values in the $\boldsymbol{S}$ and $\boldsymbol{P}$ are set equal to zero as well as those elements of $\boldsymbol{P}$ that fall outside of the concentration window. Residual standard deviation RSD

$$RSD = \sqrt{\frac{1}{N_W N_S} \sum_{i=1}^{N_W} \sum_{j=1}^{N_S} r_{ij}^2} \tag{10}$$

is calculated where r_{ij} are elements of the residual matrix

$$\boldsymbol{R} = \boldsymbol{SP}^* - \boldsymbol{A} \tag{11}$$

The iteration cycle is terminated if *RSD* falls below the stated level.

As the convergence of the iteration EFA happens to fail we have proposed to extend it by the optional direct minimization of *RSD* (eqns (*10, 11*)) with respect to the elements of the transformation matrix $\boldsymbol{T}$ (eqns (*5, 6*)). Starting $\boldsymbol{T}^0$ matrix is estimated from the relation (*5*) and from the iterative EFA results

$$\boldsymbol{T}^0 = \boldsymbol{Q}^{-1}\boldsymbol{S}(\mathrm{EFA}) \qquad (12)$$

$\boldsymbol{P}$ is calculated according to eqn (*9*) and the rules of EFA (zeroing of negative values, normalization, concentration windows) are kept working. Standard Quasi-Newton method of nonlinear optimization [12] was used for the minimization of *RSD*.

Both normalized concentration profiles and normalized component spectra are the results of EFA as well as of the proposed extension. The relation between concentration profiles and component concentrations is described by

$$\boldsymbol{\Theta P} = \boldsymbol{C} \qquad (13)$$

where $\boldsymbol{\Theta}$ is $N_C \times N_C$ diagonal matrix. The diagonal elements of this matrix are constants of the linear proportionality between components concentration profiles and components concentrations. If the total concentration of components in each mixture

$$c_j(\mathrm{total}) = \sum_{k=1}^{N_C} c_{kj} \qquad (14)$$

is known, these constants can be calculated by linear regression of eqns (*13*, *14*) and hence components concentrations and their molar absorptivity spectra can be determined.

Principal Component Regression (PCR) [13] is a multivariate calibration method utilizing the AFA decomposition of a spectral data matrix.

The reliability of the PCR calibration model can be evaluated by Cross Validation method [13, 14]. In this procedure the calibration is repeated N_R times, each time on a subset of $N_R - 1$ standards leaving one standard out. Each such subcalibration is used for prediction of the concentration of the left out standard sample. The model is characterized by the Root Mean Square Error of Cross Validation (*RMSECV*)

$$RMSECV = \sqrt{\frac{1}{N_R}\sum_{j=1}^{N_R}\left(\hat{c}_j - c_j\right)^2} \qquad (15)$$

where $\hat{c}_j$ is the predicted value and c_j is the value of concentration of the j-th left out standard, N_R is the number of the calibration standards.

The optimal value of an abstract factor space N_F can be estimated by performing the PCR modelling for several N_F values. For each N_F the value of *RMSECV* is determined and the optimal N_F corresponds to the first acceptable *RMSECV*.

RESULTS AND DISCUSSION

Keeping in dark a solution of cinnamaldehyde in methanol contains *trans*-cinnamaldehyde exclusively (checked by TLC and UV spectroscopy).

Solution of 0.078 M cinnamaldehyde in methanol was photolyzed. An oxygen stream was continuously introduced into the photolyzed solution. Set of UV absorption spectra of the 1000 diluted samples of the reaction mixtures in a certain interval of the photolysis is in Fig. 1.

TLC of the reaction mixtures has detected four components. $R_f = 0.24$ of the starting cinnamaldehyde was known. Identification of spots belonging to the *cis*-isomers ($R_f = 0.40$ for aldehyde, $R_f = 0.48$ for dimethyl acetal) was based on the observation that these spots vanish when the plate is dried with a hot air prior to development. The explanation of such disappearance is the transformation of unstable *cis*-isomers to *trans*-isomers. *Cis*-cinnamaldehyde spot was identified by its R_f known from TLC analysis of *trans-cis* photoisomerization of cinnamaldehyde (see below). The remaining spot ($R_f = 0.34$) belongs to the *trans*-dimethyl acetal of cinnamaldehyde.

Three major and three minor components were found on the GC/MS chromatogram of the reaction mixture irradiated for 600 min. Cinnamaldehyde and two isomers of dimethyl acetal of cinnamaldehyde were identified as major components according to their mass spectra. Two minor components were identified as cinnamic acid and its methyl ester while the remaining minor component was not recognized.

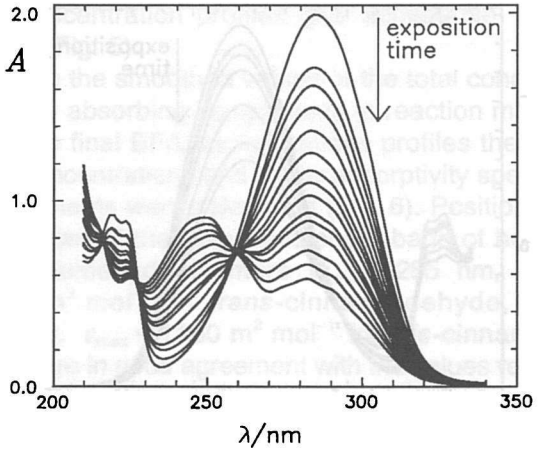

Fig. 1. Spectral set of the photooxidation of cinnamaldehyde in methanol, initial aldehyde concentrations 0.078 mol dm^{-3}, samples 1000 times diluted, 1 cm cell, exposition time/min : 0, 30, 60, 180, 270, 330, 360, 390, 420, 450, 480, 510, 540, 570, 600.

Table 1. Abstract Factor Analysis of the Spectral Set of the Reaction Mixtures of the Cinnamaldehyde Photooxidation in Methanol (A), of the Same Spectral Set with the Normalized *trans*- and *cis*-Cinnamaldehyde Spectra Added (B) and of the Spectral Set of the Reaction Mixtures of the Cinnamaldehyde Photoisomerization in Methanol (C)

N_C	*RE*		
	A	B	C
1	0.170	0.163	0.077
2	0.008	0.012	0.005
3	0.003	0.004	0.002
4	0.002	0.002	0.001
5	0.002	0.002	0.001

Results of the AFA for the spectral set of the cinnamaldehyde photooxidation reaction mixtures are in Table 1. The true experimental error for this spectral set was estimated to be not higher than 0.005. *RE* for the factor space dimension 1 and 2 is higher than this estimation while *RE* for $N_C = 3$ can be accepted as a reasonable reproduction of the experimental error. Hence AFA recognized three absorbing components in this spectral set. As the GC/MS and TLC indicate totally four components in the reaction mixtures (two isomers of cinnamaldehyde and two isomers of its dimethyl acetal) close similarity or even identity of the spectral shapes of the *trans*- and *cis*-isomers of either cinnamaldehyde or its dimethyl acetal can be presumed in this spectral region.

With the aim to study spectral properties of the *cis*-cinnamaldehyde 0.001 M cinnamaldehyde in methanol was photolyzed. An argon stream was continuously introduced into the photolyzed solution in order to lower the content of oxygen. Set of UV absorption spectra scanned during this photolysis is in Fig. 2.

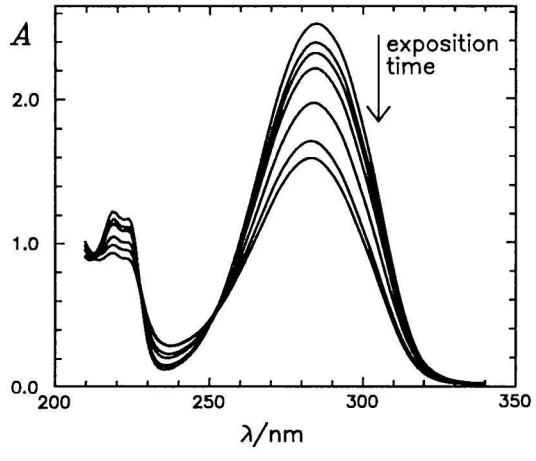

Fig. 2. Spectral set of the photoisomerization of cinnamaldehyde in methanol, initial aldehyde concentration 0.001 mol dm^{-3}, 0.1 cm cell, exposition time/s: 0, 30, 60, 90, 120, 300, 420.

GC/MS analysis of the reaction mixture after 2 h irradiation has found only two components with identical mass spectra corresponding to the *trans*- and *cis*-cinnamaldehyde. TLC has detected two components with $R_f = 0.24$ (*trans*-cinnamaldehyde) and 0.40 (*cis*-cinnamaldehyde). AFA of the spectral set of this photoisomerization indicates two absorbing components (Table 1).

The UV spectral set of the cinnamaldehyde photoisomerization in methanol was subjected to EFA. As the nonirradiated system contained *trans*-cinnamaldehyde exclusively (confirmed by TLC), its known spectrum was fixed in EFA. Primary and secondary EFA concentration profiles are in Fig. 3, EFA isolated spectrum of *cis*-cinnamaldehyde is the spectrum *b* in Fig. 6. As the total concentration of absorbing components (eqn (*14*)) is not changed in the course of photoisomerization and is equal to the initial cinnamaldehyde concentration, the concentrations of *trans*- and *cis*-cinnamaldehyde in the photoisomerization mixtures were calculated.

The normalized *trans*- and *cis*-cinnamaldehyde spectra were appended to the spectral set of the cinnamaldehyde photooxidation. AFA of such extended spectral set (Table 1) indicates that *RE* for $N_C = 3$ is the first acceptable error reproduction. As the addition of *trans*- and *cis*-cinnamaldehyde spectra does not increase the number of absorbing components these spectra must be two of the spectra recognized by AFA in the spectral set of the cinnamaldehyde photooxidation in methanol. Therefore, the third absorbing component is shared by two isomers of dimethyl acetal of cinnamaldehyde.

A quantitative analysis of reaction mixtures of the cinnamaldehyde photooxidation in methanol by a separation of the components or by any calibration method is unworkable because *cis*-cinnam-

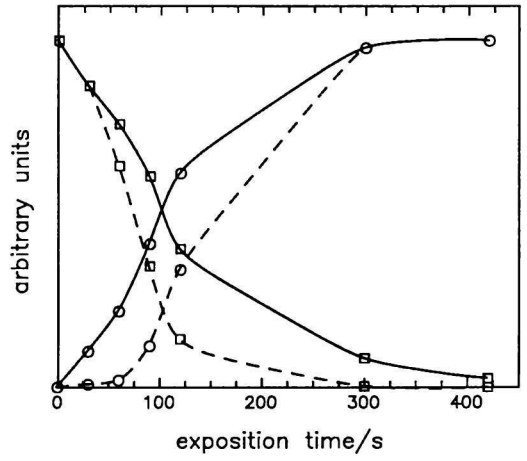

Fig. 3. Concentration profiles of the EFA analysis of the spectra of the cinnamaldehyde photoisomerization in methanol. – – – Primary EFA profiles; ——— secondary (iterative) EFA profiles; □ the first and ○ the second component.

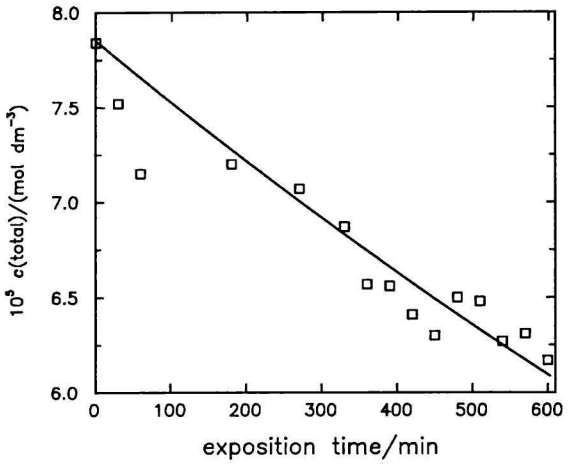

Fig. 4. Total concentration of major components during cinnamaldehyde photooxidation in methanol.

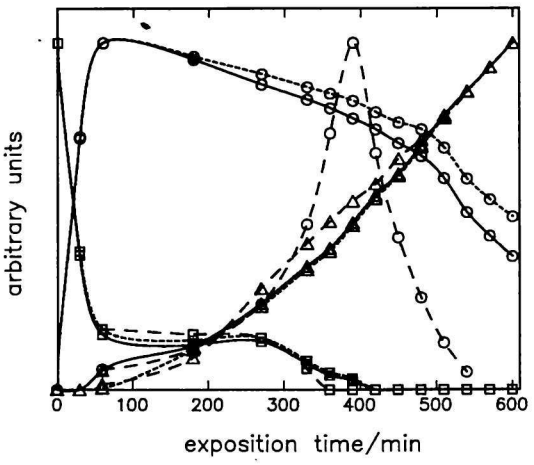

Fig. 5. Concentration profiles of the EFA analysis of the spectra of the cinnamaldehyde photooxidation in methanol. – – – Primary EFA profiles; ——— secondary (iterative) EFA profiles; - - - - - direct optimization EFA profiles; □ the first, ○ the second, and △ the third component.

aldehyde as well as dimethyl acetal of cinnamaldehyde cannot be isolated in chemically pure state and a set of standard solutions with exactly defined components concentrations cannot be prepared. *Cis*-cinnamaldehyde is unstable and changes rapidly to its *trans*-isomer. Dimethyl acetal of cinnamaldehyde is in equilibrium in methanol solution

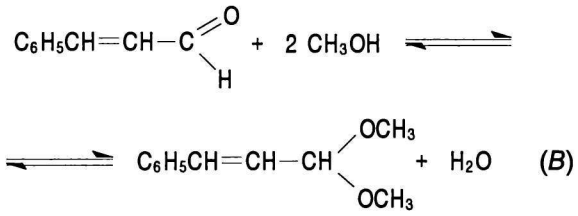

(*B*)

and ambient moisture as well as methanol evaporation shift the equilibrium towards aldehyde.

EFA is able to perform quantitative analysis of the spectral set of reaction mixtures. However, the knowledge of the total concentration of absorbing components in every mixture (eqn (*14*)) is unavoidable in order to obtain not only relative concentration profiles but also absolute concentration values. As such prolonged exposition as in the case of the cinnamaldehyde photooxidation can give rise to side reactions with side products, the total concentrations of both isomers of cinnamaldehyde and of its dimethyl acetal in reaction mixtures of cinnamaldehyde photooxidation were determined according to the following procedure.

The samples of reaction mixtures corresponding to the spectral set in Fig. 1 were separated by TLC. Plates were dried by hot air prior to development in order to change *cis*-isomers into the *trans*-ones. The spots of major components were quantitatively extracted into an acidified water. An excess of acidified water assured complete conversion of dimethyl acetal to aldehyde (eqn (*B*)). Conversion of all components to *trans*-cinnamaldehyde was checked by TLC. The amount of *trans*-cinnamaldehyde in extract corresponding to total concentration of major components was determined spectrophotometrically and normalized to conform with the dilution of samples in the spectral set of Fig. 1. The empirical smoothing function

$$c(\text{total}) = c_0 \exp[-kt] \qquad (16)$$

where t is exposition time, was fitted over these points (Fig. 5). Residual standard deviation of this approximation was 0.2×10^{-5} mol dm^{-3}.

The spectral set of cinnamaldehyde photooxidation in methanol (Fig. 1) was subjected to EFA with known spectra of *trans*- and *cis*-cinnamaldehyde fixed. As the iterations of the secondary EFA did not converge below the expected *RSD* value, the secondary EFA concentration profiles (*RSD* = 0.007) were refined by the direct minimization of *RSD*. Final concentration profiles give acceptable *RSD* = 0.005 (Fig. 5).

Using the smoothed values of the total concentrations of absorbing components in reaction mixtures and the final EFA concentrations profiles the absolute concentrations and molar absorptivity spectra of components were calculated (Fig. 6). Positions and intensities of the long wavelength band of both the cinnamaldehyde isomers (λ_{max} = 285 nm, ε_{max} = 2530 m^2 mol^{-1} for *trans*-cinnamaldehyde, λ_{max} = 283 nm, ε_{max} = 1160 m^2 mol^{-1} for *cis*-cinnamaldehyde) are in good agreement with the values reported in [15] (λ_{max} = 287 nm, ε_{max} = 2240 m^2 mol^{-1} for *trans*-cinnamaldehyde, λ_{max} = 284 nm, ε_{max} = 1260 m^2 mol^{-1} for *cis*-cinnamaldehyde).

Isolated spectrum of dimethyl acetal of cinnamaldehyde exhibits dominant peak at λ = 248 nm and two weak peaks at λ = 280—290 nm (Table 2). We have compared our data with the data estimated from not

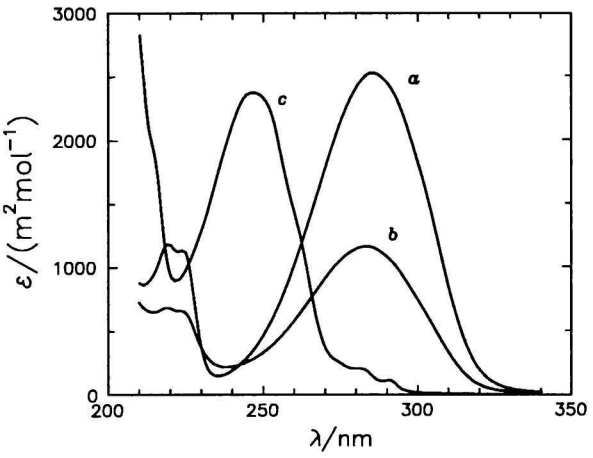

Fig. 6. Molar absorptivity spectra of the *trans*-cinnamaldehyde (*a*), *cis*-cinnamaldehyde (*b*), and cinnamaldehyde dimethyl acetal (*c*).

Table 2. Positions and Molar Absorptivities of the Peaks in the UV Spectrum of Dimethyl Acetal of Cinnamaldehyde

	λ_{max}/nm	ε_{max}/(m² mol⁻¹)
EFA (this paper)	248	2380
	280	207
	290	114
Crowell et al. [16]	251	≈ 1800
	283	≈ 250
	290	≈ 220
Fritz, Chen [17]	251	1980
	282	165
	291	120

clearly documented values of *Crowell et al.* [16] and from more recent graphical data of *Fritz* and *Chen* [17]. Spectral data [16, 17] were taken from acid-catalyzed equilibrium (*B*) shifted to the acetal side.

Based on the mixtures compositions determined by EFA the calibration model of the relation between UV spectra of cinnamaldehyde photooxidation in methanol and the concentrations of *trans*- and *cis*-cinnamaldehyde and dimethyl acetal was built by PCR. The spectral set of cinnamaldehyde photooxidation in methanol (Fig. 1) was completed with four of the spectra of cinnamaldehyde photoisomerization in methanol (Fig. 2). The optimal value of the abstract factor space N_R was found to be 4 for this model with *RMSECV* = 0.4 x 10^{-5} mol dm^{-3}. Predicted *vs.* true concentrations of individual components are in Fig. 7.

Developed calibration model will allow quantitative and kinetic analysis of the cinnamaldehyde photooxidation in methanol.

Acknowledgements: Our thanks are due to our colleagues from the Faculty of Chemical Technology of the Slovak Technical University Dr. Šurina and Dr. Vodný for GC-MS analysis.

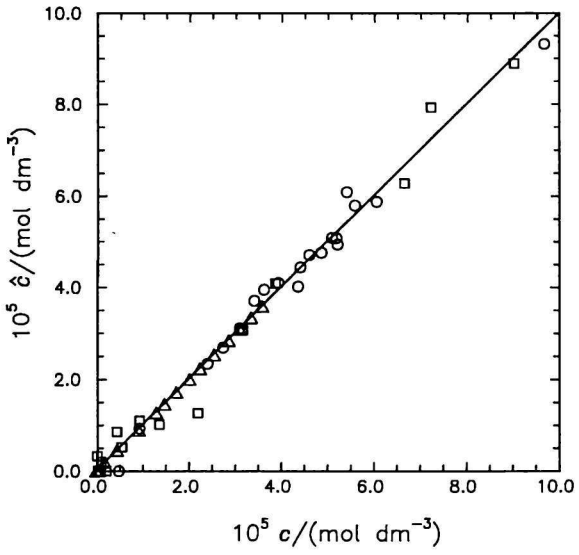

Fig. 7. Predicted *vs.* true concentration in PCR calibration model of cinnamaldehyde photooxidation in methanol. □ *trans*-Cinnamaldehyde, ○ *cis*-cinnamaldehyde, △ dimethyl acetal of cinnamaldehyde.

This study was supported by the Grant Agency for Sciences of Slovakia.

REFERENCES

1. Andre, J. C., Bouchy, M., and Niclause, M., *J. Photochem. 5*, 1 (1976).
2. Bäckström, H. L. J. and Aquist, C. F., *Acta Chem. Scand. 24*, 1431 (1979).
3. Lapčík, L., Uher, M., Valášek, J., Čeppan, M., and Blažej, A., *J. Photochem. 14*, 145 (1980).
4. Richter, F. (Editor), *Beilsteins Handbuch der Organischen Chemie,* Band *VII*. Springer-Verlag, Berlin, 1948.
5. Malinowski, E. R. , *Factor Analysis in Chemistry.* Wiley, New York, 1991.
6. Čeppan, M., Pelikán, P., and Liška, M., *Chem. Listy 85*, 1057 (1991).
7. Čeppan, M., Pelikán, P., and Liška, M., *Chem. Listy 85*, 1157 (1991).
8. Malinowski, E. R. , *Anal. Chem. 49*, 606 (1977).
9. Gamp, H., Maeder, M., Meyer, C. J., and Zuberbühler, A. D., *Talanta 33*, 943 (1986).
10. Maeder, M. and Zilian, A., *Chemometrics Intell. Lab. Systems 3*, 205 (1988).
11. Keller, H. R. and Massart, D. L., *Chemometrics Intell. Lab. Systems 12*, 209 (1992).
12. Press, W. H., Flauue, B. P., Teukolsky, S. A., and Vetterling, W. T., *Numerical Recipes.* Cambridge University Press, Cambridge, 1986.
13. Martens, H. and Naes, T., *Multivariate Calibration*, p. 97. Wiley, New York,1989.
14. Haaland, D. H. and Thomas, E. V., *Anal. Chem. 60*, 1202 (1988).
15. Gamboni, G., Theus, V., and Schniz, H., *Helv. Chim. Acta 38*, 255 (1955).
16. Crowell, E. P., Powell, W. A., and Varsel, C. J., *Anal. Chem. 35*, 184 (1963).
17. Fritz, J. S. and Chen, J., *Int. Lab. 21*, 24J (1991).

Translated by M. Čeppan